Structural Engineering and Mechanics, *Vol. 63, No. 1 (2017) 125-136*
DOI: https://doi.org/10.12989/sem.2017.63.1.125

Response of a steel column-footing connection subjected to vehicle impact

Hyungoo Kang[a] and Jinkoo Kim[*]

Department of Civil and Architectural Engineering, Sungkyunkwan University, 2066 Seobu-ro, Jangan-gu, Suwon, 440-746, Republic of Korea

(Received December 2, 2016, Revised April 24, 2017, Accepted May 10, 2017)

Abstract. This study investigated the performance of a steel column standing on a reinforced concrete footing when it was subjected to collision of an eight-ton single unit truck. Finite element analyses of the structure with different connection schemes were performed using the finite element model of the truck, and the results showed that the behavior of the column subjected to the automobile impact depended largely on the column-footing connection detail. Various reinforcement schemes were investigated to mitigate the damage caused by the car impact. The probability of the model reinforced with a certain scheme to reach a given limit state was obtained by fragility analysis, and the effects of the combined reinforcement methods were investigated based on the equivalent fragility scheme. The analysis results showed that the reinforcement schemes such as increase of the pedestal area, decrease of the pedestal height, and the steel plate jacketing of the pedestal were effective in reducing the damage. As the speed of the automobile increased the contribution of the increase in the number of the anchor bolts and the dowel bars became more important to prevent crushing of the pedestal.

Keywords: vehicle impact; FE analysis; sensitivity analysis; fragility analysis

1. Introduction

The frost line, also known as frost depth or freezing depth, is the depth to which the groundwater in soil is expected to freeze during winter season. Building codes generally take frost depth into account to prevent frost heaving which can damage buildings by moving their foundations. For this reason, foundations are normally built below the frost line in cold region. In a steel structure without basements the first story column is generally placed on a reinforced concrete (RC) pedestal or pier which is extended to the foundation located below the frost line. In columns with rigid column-footing connection, the column base plate is connected to the RC pedestal by anchor bolts designed to resist both the design gravity and lateral loads. When a vehicle collides with the first story steel column, the column-pedestal joint tends to be the weakest link in the whole structure.

Collision of a vehicle with a column has been investigated by El-Tawil *et al*. (2005) who carried out impact analysis of a bridge pier and investigated standard provisions set by the AASHTO-LRFD method for impact crash scenarios and concluded that current standards are under-conservative for bridge piers crash incidents. Itoh *et al*. (2007) simulated the progressive impact of a heavy truck on a concrete barrier, and compared the accuracy of the FEM models with full scale on-site testing results. Comparison of the results generated from computer simulations and on-site full-scale experiments demonstrated that the developed models could be applied to simulate the collision of heavy trucks with concrete barriers to provide the data to design new road safety barriers and analyze existing ones. Tsang and Lam (2008) investigated the collapse of RC columns by vehicle impact based on energy based approach. In this study the ultimate energy absorption capacity of a column is compared to the kinetic energy embodied in the moving vehicle, and the results obtained from the nonlinear static analysis were evaluated by computer simulations of the dynamic behavior of the column following the impact. The effects of strain rate were discussed and the sensitivity of the result to changes in the velocity function and stiffness of the impacting vehicle was also studied. Types of vehicle-borne threat were categorized and various considerations for mitigating vehicle-borne threats were reported in Cormie *et al*. (2009). Ferrer *et al*. (2010) carried out real size low velocity car crash experiments against a reinforced concrete building column with a rectangular section. In this paper the device, procedures and instrumentation used in these experiments were described, and it was shown that the car suffered significant plastic deformations and therefore, the use of real car in the study of low velocity impact was necessary. Joshi and Gupta (2012) investigated the plasticity induced in bridge piers with varying geometries due to a colliding vehicle by finite element analysis. They proposed a method to quantify damage in bridge piers to crash incidents, and recommendations were suggested for speed restrictions and concrete strength. Sharma *et al*. (2012) carried out performance-based response evaluation of reinforced

∗Corresponding author, Professor
E-mail: jkim12@skku.edu
[a]Ph.D.
E-mail: exult84@gmail.com

 ISSN: 1225-4568 (Print), 1598-6217 (Online)

concrete columns subject to vehicle impact to minimize damage and meet a set of performance objectives during different vehicle impact scenarios. It was found that the estimation of the dynamic shear force capacity and demand at different performance levels becomes key factor for design and protection of the structure. Tay *et al*. (2012) carried out vehicular crash test of a security bollard, and compared the results with those of numerical simulations using a finite element model for the vehicle and a force pulse generated from the impact tests. They found that the results of the two different models show good agreement. Oakes (2014) cataloged the types, costs, and performance metrics of the bollards, and recommended relevant codes and standards. Sharma *et al*. (2014, 2015) developed performance-based probabilistic models for the dynamic shear force capacity of RC columns in bridges and buildings. A framework is also developed to estimate the fragility of the RC columns subject to vehicle collision. Kang and Kim (2015) investigated the performance of three-story steel moment frames subjected to vehicle collision and compared the results with those based on the alternate path approach specified in the guidelines. The vehicle impact analysis showed that the overall damages obtained from collision analysis could be significantly larger than those obtained from the alternate path approach which was carried out by arbitrary removing of a column. Driemeier *et al*. (2016) studied the energy absorption capacity of a W-beam guardrail subjected to automobile impact. Chen *et al*. (2016) investigated progressive collapse potential of steel moment framed structures due to abrupt removal of a column based on the energy principle. Based on the changes of component’s internal energy, this paper analyzed structural member’s sensitivity to abrupt removal of a column.

According to the literature review, most of the previous studies on vehicle-column impact analysis were carried out based on the assumption that columns were rigidly fixed to the ground. This assumption may be valid in the structure with basement, where the first story columns are continuous at the joints. However, in a steel structure with its first story columns supported on reinforced concrete pedestals, the fixed bottom assumption may not be true. In this regard, this study investigates the performance of a first story steel column mounted on a RC footing subjected to vehicle collision. Special attention is paid on the effectiveness of various reinforcement schemes for reinforced concrete column pedestal supporting the steel column. The finite element model of an eight-ton single unit truck, provided by the National Transportation Research Center, is used for numerical analysis. In section 2, numerical modeling of the steel column is described. In section 3 numerical simulations of the column with different column-footing connection details subjected to vehicle collision are presented. Tornado diagram sensitivity analysis and fragility analysis are conducted to find out the relative importance of each reinforcement parameter on the response in section 4. In section 5, the performance of the structure with multiple reinforcement schemes was investigated.

2. Analysis modeling of the structure and the vehicle

2.1 Design of the model structure

The prototype structure is a three-story three-bay moment resisting frame with 6m span length. The structure is designed with dead and live loads of 7 and 6 kN/m^2, respectively, and the wind load of 137 km/h. The seismic load is computed using the design spectral acceleration coefficients SDS and SD1 of 0.67 and 0.2, respectively, based on the International Building Code (2012) format. These seismic coefficients lead to the design seismic load for structures located on class B site (rock site) in New York or Massachusetts area. To evaluate the effect of the various reinforcement methods, one of the first story corner columns is separated from the prototype structure for impact analysis as shown in Fig. 1. The column is assumed to be supported by a reinforced concrete isolated footing with a short pedestal. The story height is assumed to be 5 m in the first story, and the corner column is designed using a H-shaped section with overall dimension of 294 mm (depth)×302 (width)×12 (thickness of web)×12 (thickness of flange) made of A572 steel. The boundary conditions of the column is modeled in such a way that the bottom end is connected to the RC isolated footing, and in the top end only the horizontal displacements are restrained while all other degrees of freedom are set free as shown in Fig. 1(b). Previously similar modeling approach was applied to the impact analysis of single column by Ferrer (Ferrer et al, 2010). The foundation is composed of the 1500×1500×500 mm main body and the 500×500×600 mm pedestal on the top of the main body, which is designed using the load transmitted from the column. The placements of rebars and anchor bolts are depicted in Fig. 2, and the design parameters for the foundation are shown in Table 1.

2.2 Modeling of the vehicle

The vehicle used in the impact analysis is the eight-ton single unit truck provided by the National Transportation Research Center. The vehicle is built on a main longitudinal

Table 1 Design parameters of foundation

Base plate	Base plate	A572
	Anchor bolt	A36
	Geometry [mm]	400×400×20
Pedestal	Concrete f’c [N/mm^2]	24
	Rebar fy [N/mm^2]	400
	Main reinforcement bar	4HD19
	Hoop rebar	D10@300
	Geometry [mm]	500×500×600
Foundation	Concrete f’c [N/mm^2]	24
	Rebar fy [N/mm^2]	300
	Geometry [mm]	1500×1500×500

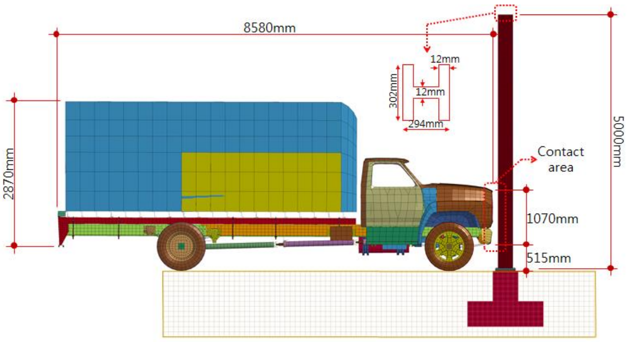

(a) Finite element models

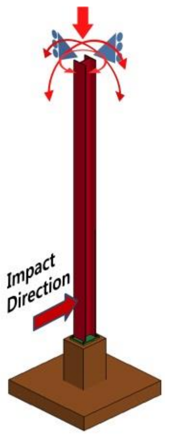

(b) Boundary condition

Fig. 1 Finite element models for single column impact simulation

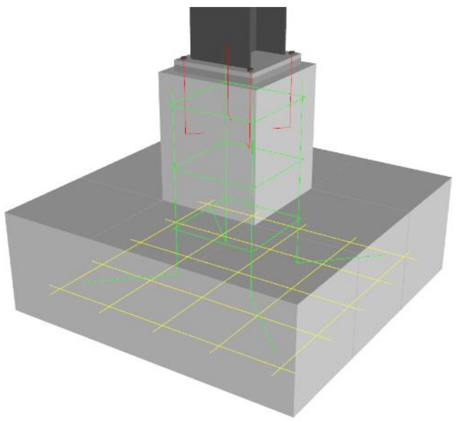

(a) 3 dimensional view

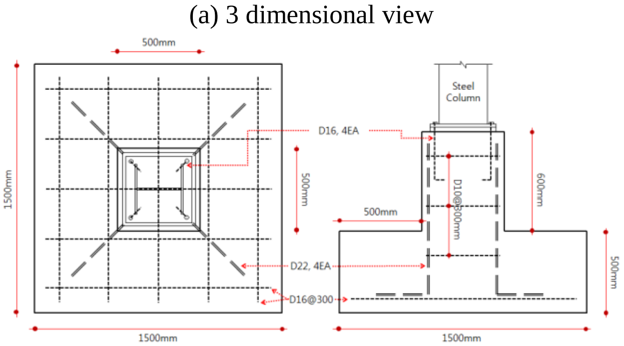

(b) Plan and elevation

Fig. 2 Rebar and anchor bolt placements in the footing-pedestal system

Table 2 Finite element model of the truck used in the impact analysis

Number of element	Shell	19,479
	Solid	1,248
	Beam	124
Weight of vehicle [kgf]		8,035
Elastic modulus [MPa]		205,000
Vehicle geometry [B×H×L, mm]		2,400×3,200×8,500

Table 3 Keywords for FE modeling

Material	Steel	*MAT_PIECEWISE_LINEAR_PLASTICITY (024)
	Concrete	*MAT_CSCM_CONCRETE (159)
	Soil	*MAT_SOIL_AND_FOAM (005)
	Ground surface	*MAT_RIGID (020)
Constrained	Rebar in concrete	*CONSTRAINED_LAGRANGE_IN_SOLID
Contact	Vehicle - Structure	*CONTACT_AUTOMATIC_SURFACE_TO_SURFACE
	Other	*CONTACT_TIED_NODES_TO_SURFACE
	Negative volume	*CONTACT_INTERIOR

rail structure that acts as its backbone. The material of the rails is specified in the Service Manual as the High Strength Low Alloy (HSLA) steel of yield point 350 MPa. The yield stress of the steel forming the surface of the truck is 155 MPa, and that of the other components is 270 MPa. The mass density and elastic modulus of steel used in the model are 7.85 kN/m^2/g and 205 GPa, respectively. It is assumed that 2.8 ton of mass is loaded on the truck, which leads to total mass of 8 ton. Table 2 shows the general information of the finite element modeling of the truck.

2.3 Modeling for finite element analysis

In this study impact analysis of a steel column is conducted using the general-purpose finite element simulation software package LS-DYNA (2006), which performs nonlinear transient dynamic analysis using explicit time integration. The steel column is modeled using the 8-node hexahedron solid elements with the elasto-plastic material named *MAT PIECEWISE LINEAR PLASTICITY, and the reinforced concrete footing and the pedestal are modeled with *MAT CSCM CONCRETE. The rebars inside of the concrete are modeled using the *CONSTRAINED LAGRANGE IN SOLID, and the soil surrounding the footing is modeled with *MAT SOIL AND FOAM. The contact condition between the structure and the vehicle is defined by the *CONTACT AUTOMATIC SURFACE TO SURFACE keyword. The friction coefficient between the ground and the wheels is assumed to be 0.01, and the ground surface is modeled by shell elements with the *MAT RIGID keyword to prevent energy dissipation due to deformation of the ground. In materials that undergo extremely large deformations, an element may become so distorted that the volume of the element may be calculated as negative. In this study, the *CONTACT INTERIOR keyword is used to prevent the occurrence of negative volume due to large deformation in the vehicle. The keywords used in the FE modeling of the structure are summarized in Table 3. Each analysis is carried out in the interval of 3.440×10^{-6} second for 0.5 sec after which the response becomes stable.

Materials can behave differently at high-speed dynamic events such as vehicle impact. In this study high strain rate effect is accounted for using the Cowper-Symonds model (Cowper *et al*. 1958) which scales the yield stress by the strain rate dependent factor as follows

$$\sigma_y = \left[1 + \left(\frac{\dot{\varepsilon}}{C}\right)^{1/p}\right]\sigma_0 \tag{1}$$

where $\dot{\varepsilon}$ is the strain rate during dynamic crushing, C and P are the Cowper-Symonds strain rate parameters. In this study the values of 40 and 5 were used for C and P, respectively, based on Liu (2011) who showed that using those values the effect of the impact velocity on the mean crushing force due to the strain rate sensitivity can be well considered in the numerical impact analysis using LS Dyna. In the impact analysis, the original yield strength σ_0 of all structural elements was replaced by the dynamic flow stress σ_y considering the strain rate effects.

2.4 Accuracy of numerical analysis

Hour glass effect is a spurious deformation mode of a Finite Element Mesh, resulting from the excitation of zero-energy degrees of freedom. Hourglass modes occur only in under-integrated (single integration point) solid, shell, and thick shell elements. LS-DYNA has various algorithms for inhibiting hourglass modes. In this study IHQ type 4 (Flanagan-Belytschko stiffness form) is used to reduce the hourglass effect. Fig. 3 shows the time history of various energy quantities of the system subjected to the vehicle collision with impact speed of 30 km/h. It is observed that the maximum ratio of the hourglass energy and the total energy is 11%, which is small enough to ensure the accuracy of the impact analysis (Zaouk *et al*. 1997).

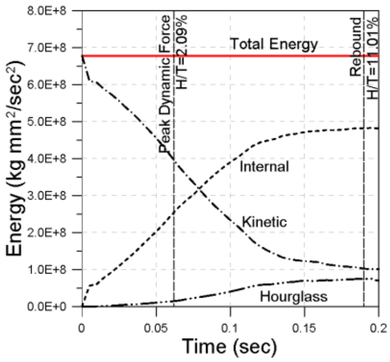

Fig. 3 Evolution of various energy quantities in the column subjected to the vehicle collision with impact speed of 30 km/h

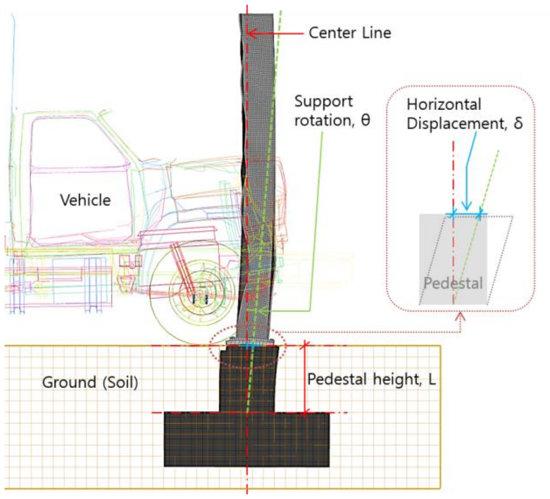

Fig. 4 Deformation of column-footing system subjected to vehicle collision

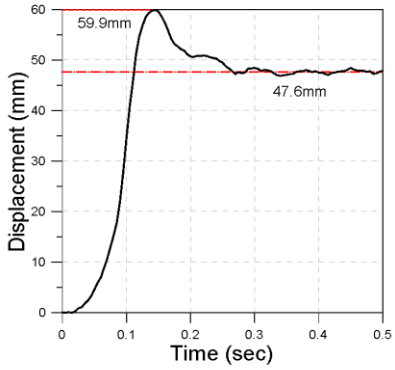

(a) Lateral displacement time history

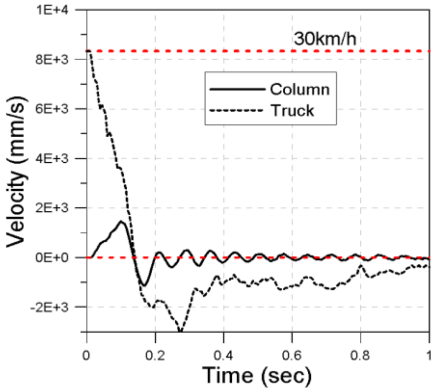

(b) Velocity time history

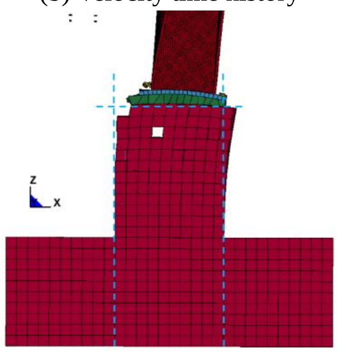

(c) Deformed configuration

Fig. 5 Response of the column pedestal subjected to the vehicle collision with impact speed of 30 km/h

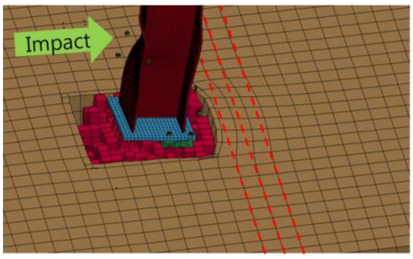

(a) Ground push out

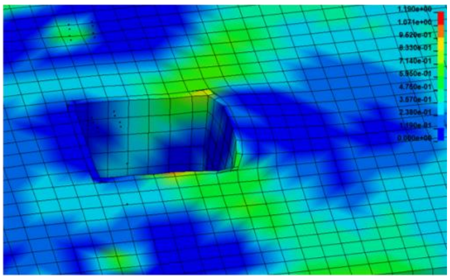

(b) Von-Mises stress distribution of ground

Fig. 6 Deformation and stress distribution of the column-pedestal and surrounding soil

3. Response of the column subjected to a vehicle impact

3.1 Damage criteria

To evaluate the damage state of a structural member, UFC (Unified Facilities Criteria, 2008) and ASCE (American Society of Civil Engineers, 2011) recommend damage limit states in terms of member rotation. In the guidelines, the limit states for the low, medium, and the high damage states are given as member rotations of 2%, 4%, and 7% radian, respectively. Fig. 4 depicts the deformation of the column-footing system when the truck collides with the column. It is estimated that the lateral displacements at the top of the pedestal corresponding to the low, medium, and the high damage states are 10.5 mm, 21.0 mm, and 41.9 mm, respectively.

3.2 Lateral displacement of the pedestal

Fig. 5 depicts the time history of the lateral displacement and velocity at the top of the pedestal and the

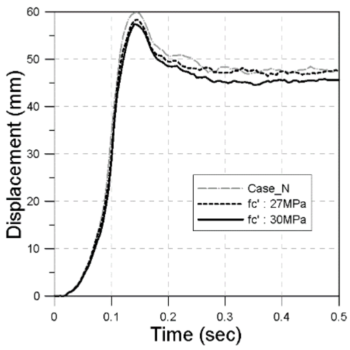

(a) Case f'c

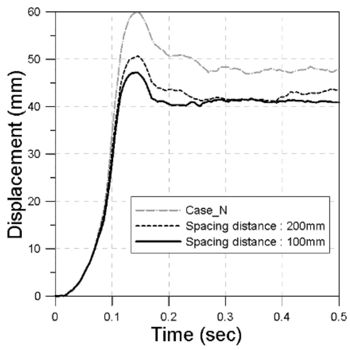

(b) Case T

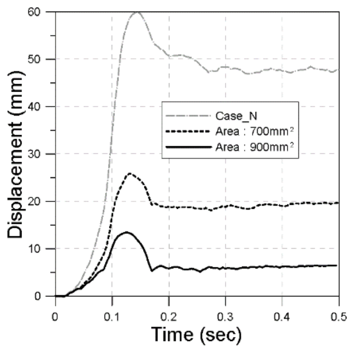

(c) Case Pa

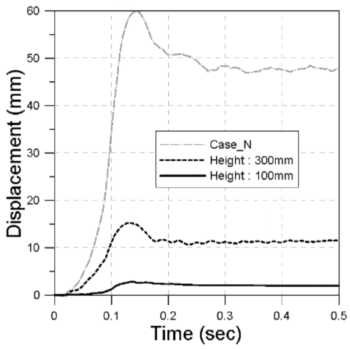

(d) Case Ph

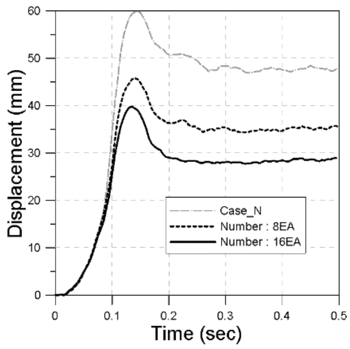

(e) Case An

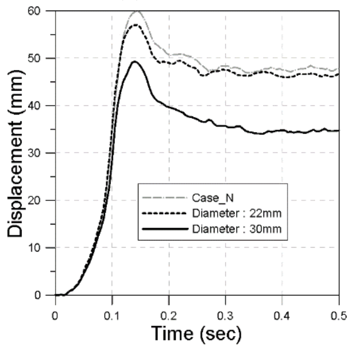

(f) Case Ad

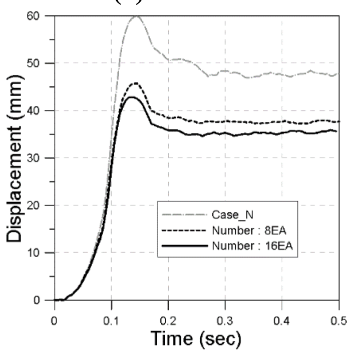

(g) Case Dn

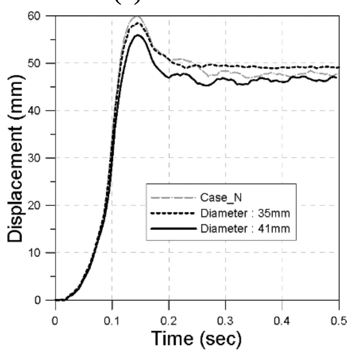

(h) Case Dd

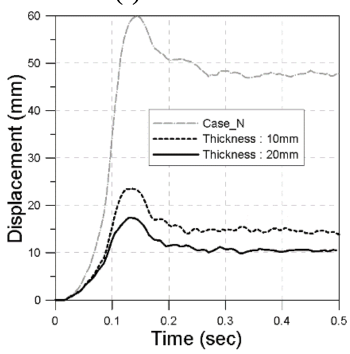

(i) Case Jt

Fig. 7 Time history of horizontal displacement (Impact velocity=30km/h)

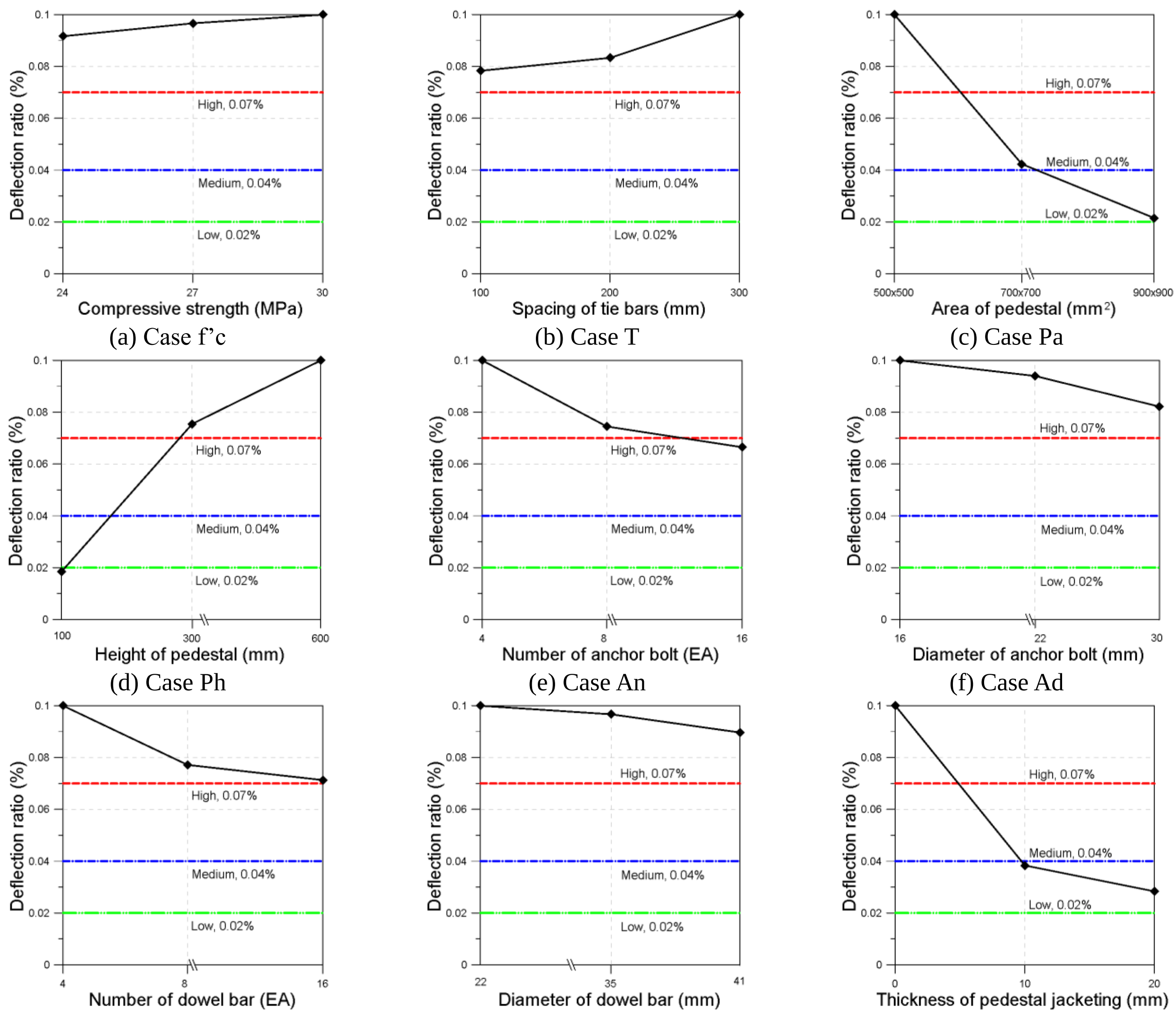

(a) Case f'c (b) Case T (c) Case Pa

(d) Case Ph (e) Case An (f) Case Ad

(g) Case Dn (h) Case Dd (i) Case Jt

Fig. 8 Maximum deflection ratio of the pedestal with various reinforcement schemes at impact velocity of 30 km/h

deformed configuration of the pedestal subjected to the vehicle collision with impact speed of 30 km/h. It can be observed that the maximum displacement reaches as high as 59.9 mm, which exceeds the high damage state specified in the guidelines. It also can be noticed that a permanent displacement of 47.6 mm remains due to the vehicle impact. Both the displacement and velocity at the top of the pedestal become stable about 0.3 second after the impact. Fig. 6 shows the deformation and stress distribution of the column-pedestal and the surrounding soil. It can be observed that due to the vehicle impact the steel column is significantly deformed and the soil surrounding the pedestal is pushed out to the direction of the impact.

3.3 Reinforcement schemes for the column-footing joint

The steel column-RC pedestal joint tends to be the weakest link of the whole system in the case of vehicle impact due to the relatively small shear strength of the anchor bolts and the pedestal. When such a system is subjected to an automobile collision the connection can be severely damaged while the column itself remains only lightly damaged. In this study various schemes are applied to reinforce the column-pedestal joint against vehicle impact, such as increase of compressive strength of concrete (Case f'c), decrease of shear rebar spacing of pedestal (Case Bd), increase of the pedestal cross sectional area (Case Pa), decrease of height of pedestal (Case Ph), increase of number (Case An) or diameter (Case Ad) of anchor bolts, increase of number (Case Dn) or diameter (Case Dd) of dowel bars for the pedestal, and jacketing of pedestal with steel plates (Case Jt).

3.4 Response of the RC pedestal reinforced with various schemes

Fig. 7 shows the time history analysis results of the column pedestal applied with nine reinforcement schemes, which are compared with the result of the original structure presented in gray dotted curve. The impact speed is set to be 30 km/h at which complete separation of the column from

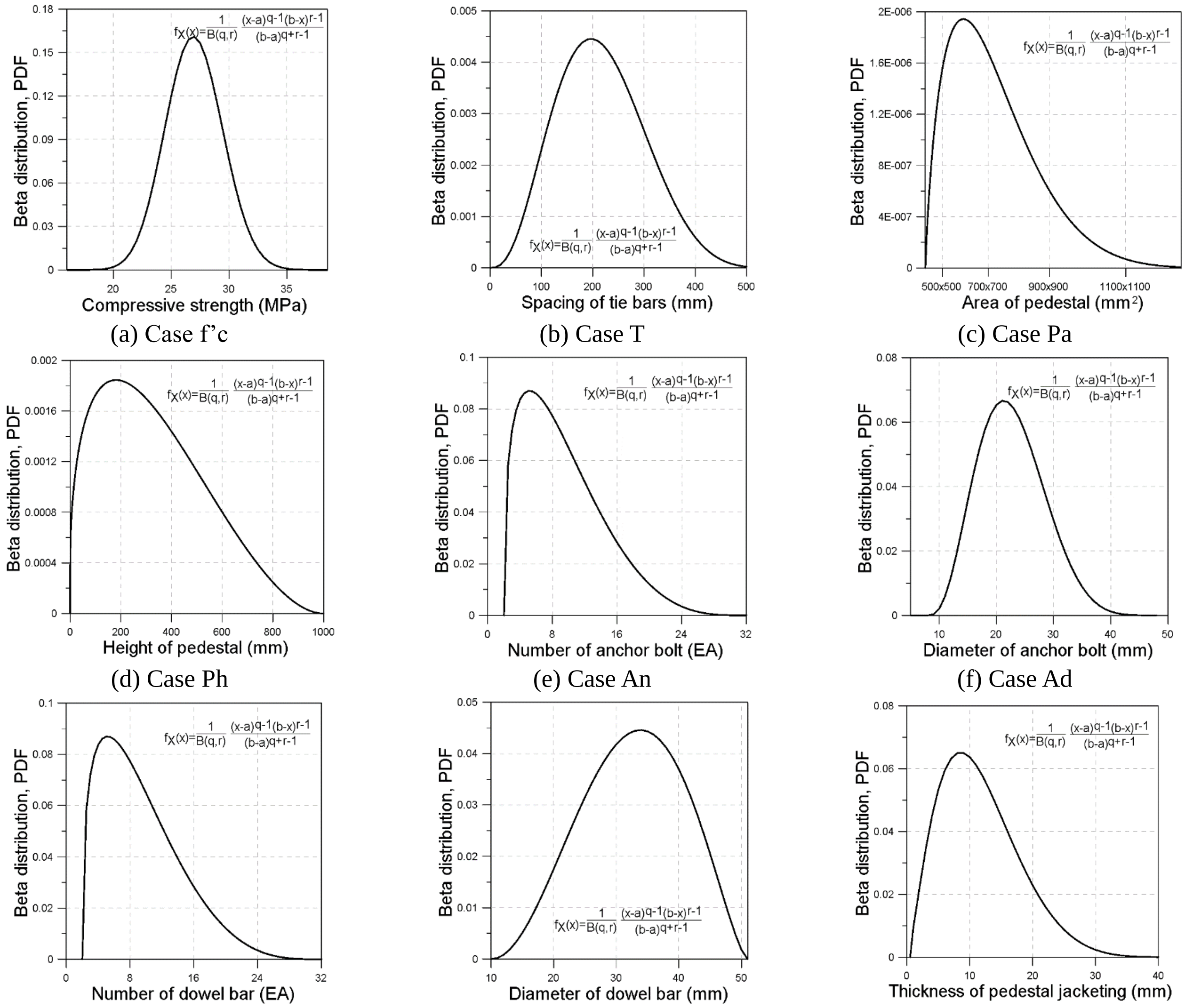

(a) Case f'c (b) Case T (c) Case Pa

(d) Case Ph (e) Case An (f) Case Ad

(g) Case Dn (h) Case Dd (i) Case Jt

Fig. 9 Statistical distribution of retrofit parameters

the pedestal does not happen. The reinforcement of the pedestal is made in practically reasonable range of design parameters. For each reinforcement scheme two different levels of reinforcement are applied while the other design variables remain unchanged from the original design. It can be observed that the effectiveness of the reinforcement schemes increases in the order of Case f'c, Case Dd, Case Ad, Case Bd, Case Dn, Case An, Case Jt, Case Pa, and Case Ph.

Fig. 8 shows the maximum deflection ratio of the pedestal with various design parameters due to the impact. For example, the deflection ratio of 1% corresponds to the support rotations of 1.14°. It can be observed that the response of the pedestal is reduced below the Medium damage state only in the design parameter cases Pa, Ph, and Jt.

4. Probabilistic evaluation of the column pedestal under impact load

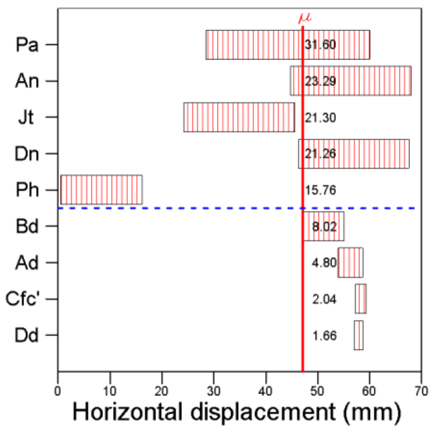

Fig. 10 Tornado diagram of displacement for various reinforcement methods

4.1 Sensitivity analysis

A sensitivity analysis is a technique used to determine how different values of an input variable will impact a particular output value under a given set of assumptions. Miyamoto and Isoda (2012) carried out a sensitivity analysis for rational health monitoring of bridges. In this study Tornado diagram analysis (TDA), which is one of the sensitivity analysis tools commonly used in decision analysis, is carried out to find out the relative sensitivity of each design variable of a column pedestal when the column is subjected to an automobile impact. In TDA, the upper and lower bounds of the parameters are selected as $\pm 1/2\sigma$, where σ is the standard deviation, and the corresponding structural responses are obtained. The difference between such structural responses, referred to as swing, is considered as a measure of sensitivity. Porter *et al*. (2002) applied it to the seismic sensitivity analysis of structures, and Kim *et al*. (2011) carried out sensitivity analysis of steel buildings subjected to column loss using three different methods including TDA.

To carry out statistical analysis of the column-pedestal system reinforced with various schemes, the statistical distribution of each design variable is constructed using the beta distribution function based on the data available in practice as shown in Fig. 9. As there are definite upper and low bounds in the possible range of variation of the variables considered in the reinforcement, the beta distribution is suitable for probabilistic distribution of the design variables for the pedestal. Fig. 10 shows the tornado diagrams of the displacement plotted for each of the reinforcement method in the order of swing size. The vertical line denotes the mean displacement. It can be observed that the swing is largest when the horizontal dimension of the pedestal is varied (Case Pa), followed by the variation of the number of anchor bolts (Case An) and the thickness of the steel plate jackets (Case Jt). The effects of variations in the compressive strength of concrete (Case f’c) and the diameter of anchor bolts (Case Ad) and dowel bars (Case Dd) turn out to be insignificant. The reinforcement schemes Case Jt and Case Ph result in small displacement compared with the other schemes.

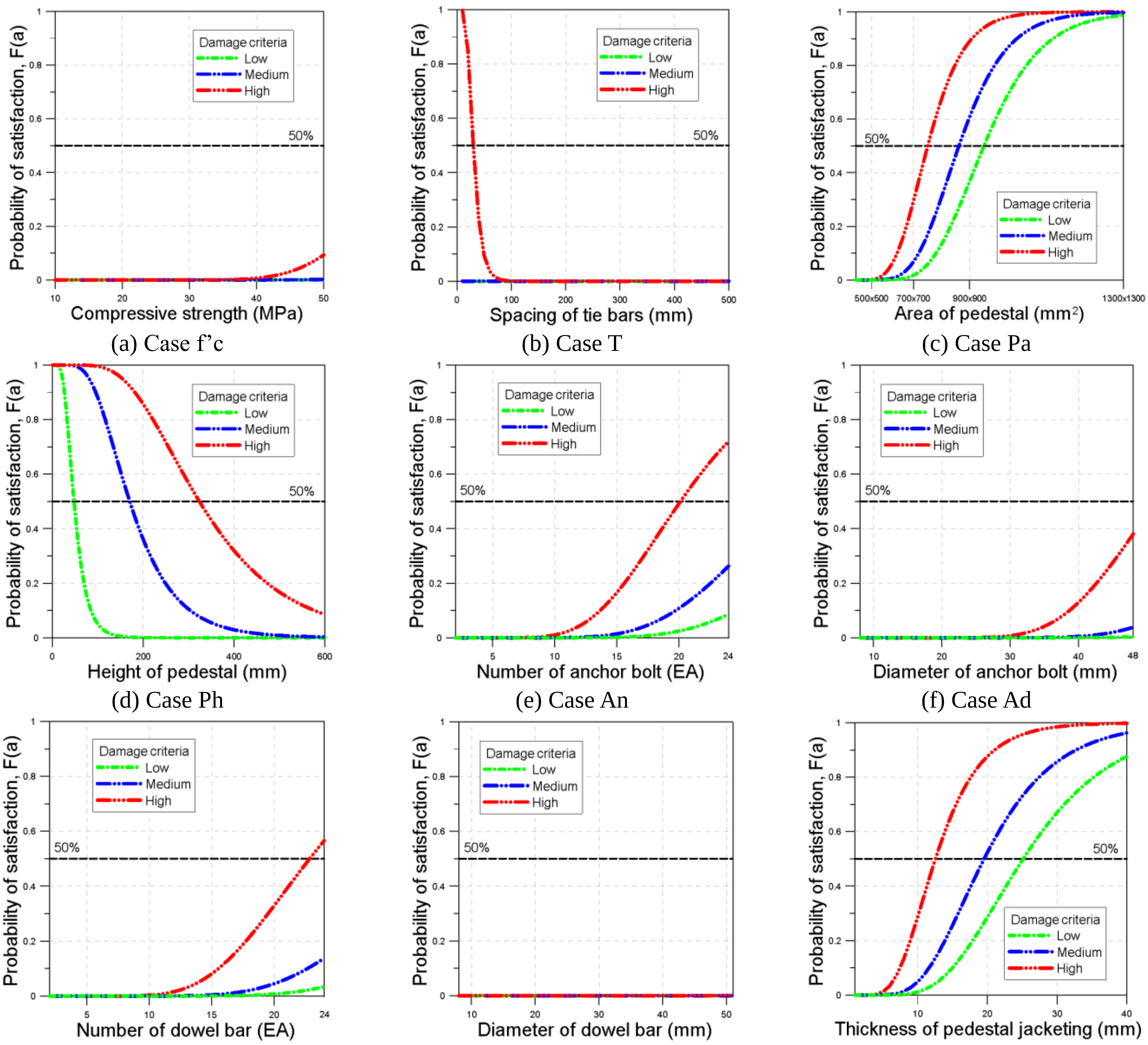

(a) Case f’c (b) Case T (c) Case Pa

(d) Case Ph (e) Case An (f) Case Ad

(g) Case Dn (h) Case Dd (i) Case Jt

Fig. 11 Probability of satisfaction curve for various reinforcement methods at impact velocity of 30km/h

4.2 Fragility analysis

Fragility analysis is generally carried out to estimate the probability of reaching a limit state at a given design parameter value (Shinozuka *et al*. 2000). Even though such technique is generally applied in seismic engineering, it is also used for other engineering fields. For example, Jurewicz *et al*. (2016) carried out fragility analysis of a safety system to investigate the relationship between the automobile speed and injury of pedestrians. Sharma *et al*. (2014, 2015) developed performance-based probabilistic models and fragility curves for the dynamic shear force capacity of RC columns. Lee *et al*. (2016) applied fragility analysis procedure to study the reliability of bridges against flood.

In this study, it is assumed that the probability distribution of the reinforcement parameters is expressed in the form of beta distribution functions, and the estimations of the median and the standard deviation are performed with the aid of the maximum likelihood method. The likelihood function for the present purpose is expressed as

$$P(x\,|\,\theta) = \prod_{i=1}^{N}[F(a_i)]^{x_i}[1-F(a_i)]^{1-x_i} \qquad (2)$$

where $F(\bullet)$ represents the fragility curve for a specific state of damage; a_i is the ith value of a reinforcement parameter, N is the total number of parameter values, x_i is 1 or 0 depending on whether or not the damage state is over. The function F(a) has a form as follows

$$F(a) = \Phi\left[\frac{ln\frac{a}{c}}{\varsigma}\right] \qquad (3)$$

where Φ[•] is the probability distribution function, c is the median value of the parameters which satisfy the given damage criterion, and ζ is the standard deviation of the parameter values. The parameters c and ζ which maximize the likelihood function (L) can be obtained using the following equation

$$L = \prod_{i=1}^{N}[F(a_i)]^{x_i}[1-F(a_i)]^{1-x_i} \qquad (4)$$

$$\frac{dlnL}{dc} = \frac{dlnL}{d\varsigma} \qquad (5)$$

The probability density functions depicted in Fig. 9 is substituted to Eq. (3) to construct fragility curves.

To evaluate the probability of reaching a given damage limit state of the column when it is subjected to vehicle collision, fragility curves are drawn in Fig. 11. In the figure, the probability of satisfaction, which is the inverse of the probability of reaching the limit sate, is plotted as a function of the design variables (capacities). Reaching the value of 1.0 in the vertical axis implies that the probability of reaching the given limit state is zero. It can be observed that Case Pa, Case Ph, and Case Jt satisfy 50% of the probability of satisfying all of the three low, medium, and high damage states. It also can be observed that Case An, Case Dn, and Case Bd reach the 50% satisfaction probability only for the high damage state. In the reinforcement Cases f’c and Dd, the variation of a design variable has only a small possibility to satisfy the given limit state when it is varied within a given range. In these cases the reinforcement methods have only a minute effect in decreasing the displacement of the column capital subjected to an automobile impact.

5. Performance of the structure with multiple reinforcement schemes

In this section, five reinforcement schemes which turn out to be relatively effective in the fragility analysis are selected and are combined to effectively reinforce the pedestal. The parameter values having 10, 30, and 50% probabilities of satisfying each limit state are shown in Table 4. For example, the thickness of the steel jacket plates needs to be 13 mm and 25 mm, respectively, for 50% satisfaction probability of the high and the low damage states. In the case of the number of dowel bars, there is no design value within the given range of variation which satisfies the low damage state with 30 and 50% of satisfaction.

Fig. 12 shows the impact analysis results of the model structure reinforced with combined schemes subjected to the automobile impact with 30 km/h speed. The reinforcement parameters are determined as the values which have 10% probability of satisfying the high damage state obtained from the fragility analysis, and impact analysis is carried out with various combinations of

Table 4 Design parameter values for given probability of satisfaction

Retrofit cases	Unit	Unreinforced value	Design parameter values for X% satisfaction probability								
			50%			30%			10%		
			Low	Medium	High	Low	Medium	High	Low	Medium	High
Case Pa	cm^2	500	943	866	754	877	806	700	787	721	624
Case Ph	Mm	600	45	170	325	60	215	410	85	300	575
Case An	-	4	*	29	20	31	25	17	25	20	14
Case Dn	-	4	*	*	23	*	28	19	28	23	16
Case Jt	mm	0	25	20	13	21	16	10	15	12	8

* No value for satisfying the damage limit state within the given range

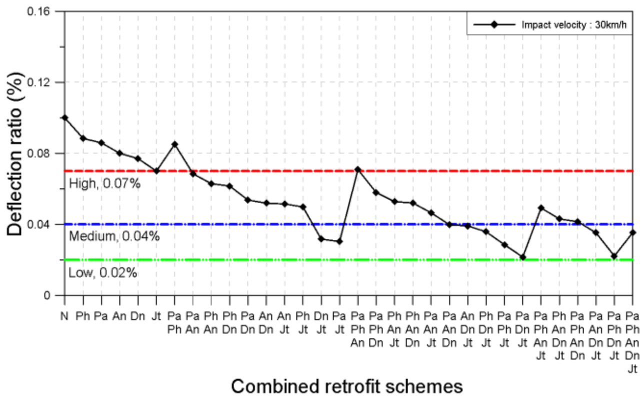

Fig. 12 Deflection ratio of the pedestal with combined reinforcement schemes at 30km/h impact speed

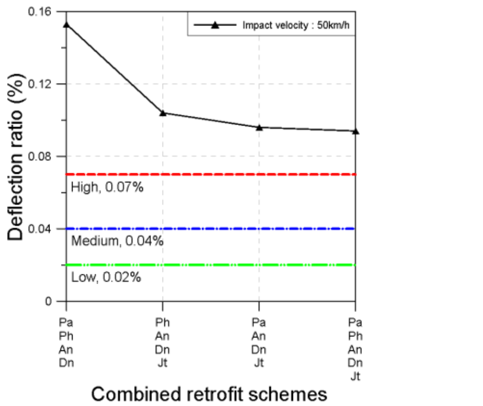

Fig. 13 Deflection ratio of pedestal with combined reinforcement schemes at 50 km/h impact speed

reinforcement methods. It is observed that a single reinforcement method results in a response above the high damage state. In the figure, it can be observed that the simultaneous application of two reinforcement methods generally leads to responses between the high and the medium damage states. About half of the responses of the structure with combinations of three reinforcement methods are between the high and the medium damage states, and half of the responses with combinations of four reinforcement methods are between the medium and the low damage states. Generally, the combination of parameters including the jacketing of pedestal (Case Jt) results in relatively smaller response.

In case the velocity of the automobile is increased to 40m/h, the column is completely severed from the pedestal when the increase of the number of anchor bolts is not included in the reinforcement scheme. It is observed that the reinforcement methods associated with the reduction of pedestal height (case Ph), increase of the parameters such as pedestal area (Pa)/ dowel bars (Dn)/ anchor bolts (An), and the addition of steel plate jackets (Jt) result in relatively low responses. The damaged configuration of the pedestal and the footing shows that significant damage occurs in the pedestal in case jacketing is not provided. Figure 13 depicts the deflection ratio of the pedestal retrofitted with combined reinforcement schemes at 50km/h impact speed. In this case, at least four reinforcement schemes need to be combined to prevent the total failure of the pedestal due to the impact. Even though most retrofit cases resulted in response above the medium or even high damage limit state, the column still has redundant capacity against collapse. It is also observed that the reinforcement of anchor bolts (Case An) and dowel bars (Case Dn) need to be included in the reinforcement schemes to prevent complete failure. The inclusion of steel plate jacketing (Case Jt) results in significant reduction of the response. However, even with application of four or five reinforcement schemes, the response still exceeds the high damage state.

Fig. 14 shows the recommended detail of the reinforced footing pedestal, and Fig. 15 depicts the damaged configuration of the system subjected to the automobile collision with impact speed of 50 km/h, where it is found that with the four reinforcement schemes (Case Ph + An +

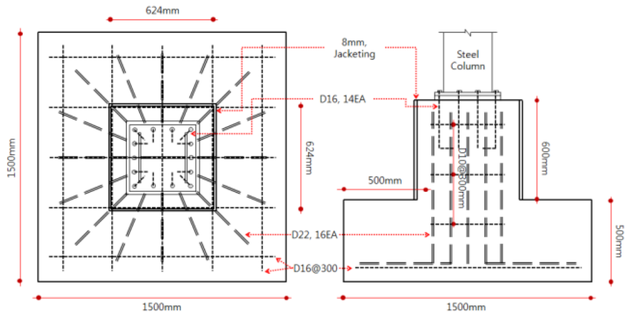

Fig. 14 Recommended detail of the reinforced footing pedestal (Case Ph + An + Dn + Jt)

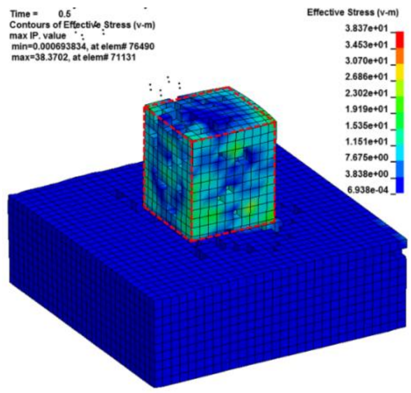

(a) Case Ph + An + Dn + Jt

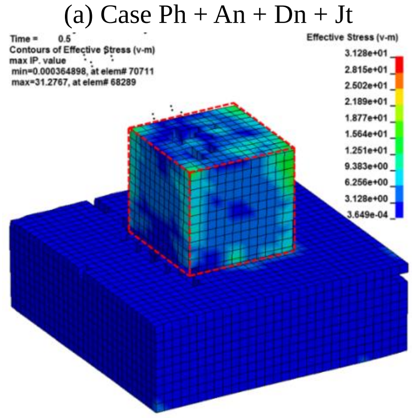

(b) Case Pa + Ph + An + Dn + Jt

Fig. 15 Damaged configuration of the footing-pedestal system with various retrofit schemes subjected to vehicle collision with 50 km/h impact speed

Dn + Jt) slight damage is observed in the pedestal. It also can be observed that after including one more reinforcement scheme (Case Pa) the damage in the pedestal disappears.

6. Conclusions

In this study the performance of a steel column standing on a reinforced concrete footing subjected to a vehicle collision was investigated. According to the sensitivity analysis, the reinforcement schemes involved with the height and cross sectional area of the pedestal, the number of anchor bolts and dowel bars, and the steel plate jacketing turned out to affect the response most significantly. The analysis of the structure subjected to the low speed impact of the vehicle showed that the reinforcement schemes such as increase of the pedestal area, decrease of the pedestal height, and the steel plate jacketing of the pedestal are effective in reducing the response below the medium damage state. When the impact speed increased to 40~50 km/h, the contribution of the increase in the number of the anchor bolts and the dowel bars became more important to prevent shearing of anchor bolts and crushing of pedestal. It was also observed that the safety of the column-footing system could be greatly enhanced by applying appropriately combined multiple reinforcement schemes for the pedestal. Based on the analysis results the design details and response of some recommended retrofit cases were presented such as retrofit with additional anchor bolts, dowel bars, plate jacketing and changing the cross-sectional area and height of the pedestal.

As huge amount of computation was required for statistical analysis in this study, only the most basic elements such as the column, footing, and the soil were included in the finite element modeling. The results of this study may have been different if more realistic three-dimensional analysis model with accurate boundary conditions was used instead of the single column on a footing model used in this study. It also needs to be mentioned that the column of the model structure is rigidly connected to the RC pedestal, and the pin connection may behave differently.

Acknowledgments

This research was supported by Basic Science Research Program through the National Research Foundation of Korea (NRF) funded by the Ministry of Education (NRF-2016R1D1A1B03932880).

References

ASCE/SEI 59-11 (2011), Blast protection of buildings, American Society of Civil Engineers.

Chen, C.H., Zhu, Y.F., Yao, Y. and Huang, Y. (2016), "Progressive collapse analysis of steel frame structure based on the energy principle", *Steel Compos. Struct.*, **21**(3), 553-571.

Cormie, D., Mays, G. and Smith, P. (2009), *Blast effects on buildings (2nd edition)*, Thomas Telford Limited, UK.

Cowper, G.R. and Symonds, P.S. (1957), *Strain-hardening and strain-rate effects in the impact loading of cantilever beams (No. TR-C11-28)*, Brown Univ Providence Ri.

Driemeier, L., Yoneda, A., Moura, R.T. and Alves, M. (2016), "Performance of metallic defences submitted to vehicle impact", *Int. J. Crashworthiness*, **21**(3), 252-277.

El-Tawil, S., Severino, E. and Fonseca, P. (2005), "Vehicle collision with bridge piers", *J. Bridge Eng.*, **10**(3), 345-353.

Ferrer, B., Ivorra, S., Irles, R. and Mas, D. (2010), "Real size experiments of car crash against building column", *Structures Under Shock and Impact XI*, Wessex Institute of Technology, UK, 231-241.

International Building Code (IBC) (2012), International Code Council.

Itoh, Y., Liu, C. and Kusama, R. (2007), "Dynamic simulation of collisions of heavy high-speed trucks with concrete barriers", *Chaos, Soliton. Fract.*, **34**(4), 1239-1244.

Joshi, A.S. and Gupta, L.M. (2012), "A simulation study on quantifying damage in bridge piers subjected to vehicle collisions", *Int. J. Adv. Struct. Eng. (IJASE)*, **4**(1), 1-13.

Jurewicz, C., Sobhani, A., Woolley, J., Dutschke, J. and Corben, B. (2016), "Exploration of vehicle impact speed-injury severity relationships for application in safer road design", *Transport. Res. Procedia*, **14**, 4247-4256.

Kang, H. and Kim, J. (2015), "Progressive collapse of steel moment frames subjected to vehicle impact", *J. Perform. Constr. Facil.*, **29**(6), 1-11.

Kim, J., Park, J. and Lee, T. (2011), "Sensitivity analysis of steel buildings subjected to column loss", *Eng. Struct.*, **33**(2), 421-432.

Lee, J., Lee, Y.J., Kim, H., Sim, S.H. and Kim, J.M. (2016), "A new methodology development for flood fragility curve derivation considering structural deterioration for bridges", *Smart Struct. Syst.*, **17**(1), 149-165.

Liu, Y. (2011), "Study of thin-walled box beams crushing behavior using LS-DYNA", *11th International LS-DYNA® Users Conference*, **13**, 31-40.

LS-DYNA (2006), *Theory manual version 971*, © Livemore Software Technology Corporation.

Miyamoto, A. and Isoda, S. (2012), "Sensitivity analysis of mechanical behaviors for bridge damage assessment", *Struct. Eng. Mech.*, **41**(4), 539-558.

NTRCI (2017), National Transportation Research Center, http://thyme.ornl.gov/fhwa/f800webpage/.

Oakes, C.G (2014), *The Bollard: Crash- and Attack-Resistant Models*, Whole Building Design Guide, The National Institute of Building Sciences.

Porter, K.A., Beck, J.L. and Shaikhutdinov, R.V. (2002), "Sensitivity of building loss estimates to major uncertain variables", *Earthq. Spectra*, **18**(4), 719-743.

Sharma, H., Gardoni, P. and Hurlebaus, S. (2014), "Probabilistic demand model and performance-based fragility estimates for RC column subject to vehicle collision", *Eng. Struct.*, **74**, 86-95.

Sharma, H., Gardoni, P. and Hurlebaus, S. (2015), "Performance-based probabilistic capacity models and fragility estimates for RC columns subject to vehicle collision", *Comput.-Aid. Civ. Infrastruct. Eng.*, **30**(7), 555-569.

Sharma, H., Hurlebaus, S. and Gardoni, P. (2012), "Performance-based response evaluation of reinforced concrete columns subject to vehicle impact", *Int. J. Impact Eng.*, **43**(5), 52-62.

Shinozuka, M., Feng, M. Q., Lee, J. and Naganuma, T. (2000), "Statistical analysis of fragility curves", *J. Eng. Mech.*, **126**(12), 1224-1231.

Tay, S.K., Lim, B. and Ng, S.H. (2012), "Crash impact modeling of security bollard", *12th International LS-DYNA® Users Conference*, **13**, 1-10.

Tsang, H.H. and Lam, N.T.K. (2008), "Collapse of reinforced concrete column by vehicle impact", *Comput.-Aid. Civ. Infrastruct. Eng.*, **23**(6), 427-436.

Unified facilities criteria (UFC) 3-340-02 (2008), *Structures to resist the effects of accidental explosions*, U.S. Department of Defense.

Zaouk, A.K., Bedewi, N.E., Kan, C.D. and Marzougui, D. (1997), *Development and evaluation of a C-1500 pick-up truck model for roadside hardware impact simulation*, FHWA/NHTSA National Crash Analysis Center, The George Washington University, July.

PL